Original Article

Fast dual-echo estimation of apparent long T2 fraction using ultrashort echo time magnetic resonance imaging in tibialis tendons and its osteoporosis-related differences in women

Saeed Jerban[1,2,3#], Dina Moazamian[1#], Yajun Ma[1,2], Amir Masoud Afsahi[1], Sophia Dwek[1], Jiyo Athertya[1], Bhavsimran Malhi[1], Hyungseok Jang[1,2], Gina Woods[4], Christine B. Chung[1,2], Jiang Du[1,2], Eric Y. Chang[1,2]

[1]Department of Radiology, University of California, San Diego, La Jolla, CA, USA; [2]Research Service, Veterans Affairs San Diego Healthcare System, San Diego, La Jolla, CA, USA; [3]Department of Orthopaedic Surgery, University of California, San Diego, La Jolla, CA, USA; [4]Department of Medicine, University of California, San Diego, La Jolla, CA, USA

Contributions: (I) Conception and design: EY Chang, S Jerban, J Du, Y Ma, CB Chung; (II) Administrative support: CB Chung, J Du, EY Chang; (III) Provision of study materials or patients: S Jerban, G Woods, H Jang; (IV) Collection and assembly of data: AM Afsahi, Y Ma, S Jerban, D Moazamian, S Dwek, J Athertya, B Malhi; (V) Data analysis and interpretation: D Moazamian, S Dwek, AM Afsahi, S Jerban, J Athertya; (VI) Manuscript writing: All authors; (VII) Final approval of manuscript: All authors.

[#]These authors contributed equally to this work.

Correspondence to: Eric Y. Chang, MD. Department of Radiology, University of California, Radiology Service, Veterans Affairs San Diego Healthcare System, 3350 La Jolla Village Drive, San Diego, CA 92161, USA. Email: eric.chang2@va.gov; Saeed Jerban, PhD. Department of Radiology, University of California, San Diego, La Jolla, CA, USA; Research Service, Veterans Affairs San Diego Healthcare System, San Diego, La Jolla, CA, USA; Department of Orthopaedic Surgery, University of California, 9500 Gilman Dr., San Diego, CA 92093, USA. Email: sjerban@health.ucsd.edu; Dina Moazamian, MD. Department of Radiology, University of California, 9500 Gilman Dr., San Diego, CA 92093, USA. Email: dmoazamian@health.ucsd.edu.

Background: Tendon and bone comprise a critical interrelating unit. Bone loss, including that seen with osteopenia (OPe) or osteoporosis (OPo), may be associated with a reduction in tendon quality, though this remains incompletely investigated. Clinical magnetic resonance imaging (MRI) sequences cannot directly detect signals from tendons because of the very short T2. Clinical MRI may detect high-graded abnormalities by changes in the adjacent structures like bone. However, ultrashort echo time MRI (UTE-MRI) can capture high signals from all tendons. To determine if the long T2 fraction, as measured by a dual-echo UTE-MRI sequence, is a sensitive quantitative technique to the age- and bone-loss-related changes of the lower leg tendons.

Methods: This is a cross-sectional study conducted between January 2018 to February 2020 in the lower legs of 14 female patients with OPe [72±6 years old, body mass index (BMI) =25.8±6.2 kg/m^2] and 31 female patients with OPo (73±6 years old, BMI=22.0±3.8 kg/m^2), as well as 30 female subjects with normal bone (Normal, 35±18 years old, BMI =23.2±4.3 kg/m^2), were imaged on a 3T clinical scanner using a dual-echo 3D Cones UTE sequence. We defined the apparent long T2 signal fraction (aFrac-LongT2) of tendons as the ratio between the signal at the second echo time (TE =2.2 ms) to the UTE signal. The average aFrac-LongT2 and the cross-sectional area were calculated for the anterior tibialis tendons (ATTs) and the posterior tibialis tendons (PTTs). The Kruskal-Wallis rank test was used to compare the differences in aFrac-LongT2 and the cross-sectional area of the tendons between the groups.

Results: The aFrac-LongT2 of the ATTs and PTTs were significantly higher in the OPo group compared with the Normal group (22.2% and 34.8% in the ATT and PTT, respectively, P<0.01). The cross-sectional area in the ATTs was significantly higher for the OPo group than in the Normal group (Normal/OPo difference was 28.7, P<0.01). Such a difference for PTTs did not reach the significance level. Mean aFrac-LongT2 and cross-sectional area in the OPe group were higher than the Normal group and lower than the

OPo group. However, the differences did not show statistical significance, likely due to the higher BMI in the OPe group.

Conclusions: Dual-echo UTE-MRI is a rapid quantification technique, and aFrac-LongT2 values showed significant differences in tendons between Normal and OPo patients.

Keywords: Tibialis tendon; tendon quality; osteoporosis (OPo); magnetic resonance imaging (MRI); ultrashort echo time

Submitted Sep 19, 2023. Accepted for publication Jan 09, 2024. Published online Mar 15, 2024.
doi: 10.21037/qims-23-1341
View this article at: https://dx.doi.org/10.21037/qims-23-1341

Introduction

Tendon and bone are complementary tissues that comprise a critical interrelating unit for body movement and autonomy (1). In such a mechanical unit, bone performs as a lever for skeletal muscle force transferred by the tendon. The generated force by muscle contractions is applied to bone (1,2) and tendon (3) and influences their strength and microarchitecture. For example, Chen *et al.*, have shown that bone mineral density significantly correlates with the tendon's mechanical strength in rabbit model (4). Besides the mechanical connections, biochemical and metabolic interactions between bone and tendon significantly impact their quality and function (5). Systemic anabolic and catabolic hormone levels and molecules as well as the inflammatory cytokine activity can affect cell activity in both tendon and bone (6-9).

Bone loss in osteoporosis (OPo) which define as Dual-Energy X-ray Absorptiometry (DXA) T-scores below –2.5 and in its earlier stage disease, osteopenia (OPe) which define as DXA T-scores between –2.5 and –1 in the clinical approaches, may be linked with the tendon quality decline (7,10-12). Evaluation of the quality of tendons during the disease progression using quantitative noninvasive methods is of critical interest to the research community. Such evaluations of tendons can help to enhance our understanding of OPo and may eventually improve the management and treatment of the disease.

The gold standard for confirming tendinopathy in the anterior tibialis tendon (ATT) would be ultrasonography, because of its accessibility and affordability (13,14). However, for the posterior tibialis tendon (PTT), ultrasonography may encounter challenges due to the tissue depth and bone proximity.

Magnetic resonance imaging (MRI) is regularly used for the diagnosis of frank tendon tearing (10,11,15), but clinical MRI techniques encounter challenges in the detection of more subtle abnormalities (16-18). Intact tendons possess very short spin-spin (T2) relaxation times due to highly organized collagenous matrix (16). When imaged using conventional MRI sequences, the resultant low signal-to-noise ratio precludes the accurate differentiation between healthy tendons and grossly intact but abnormal tissue (19).

Contrary to conventional MRI sequences, ultrashort echo time (UTE) MRI techniques can detect a considerable signal from both the short T2 (e.g., bound water to tendon fibers) and long T2 (e.g., free water and potential endotenon fat) components in tendons (16). Consequently, UTE-MR imaging is capable of providing robust image-based biomarkers for quantitative of tendon assessment (16,20-22). The quantitative ultrashort echo time MRI (UTE-MRI)-based evaluation of tendons in clinical studies has been challenging partly caused by the high cost and time demands of MRI in general. Therefore, developing more rapid quantitative UTE-MRI techniques is expected to facilitate the inclusion of UTE sequences in clinical studies for tendon evaluation.

The fraction of the long T2 component (Frac-LongT2) in tendons can be calculated by the signal ratio in dual-echo UTE imaging (23) which is a remarkable example of rapid UTE-based techniques which can be performed in less than 5 minutes. As mentioned, the UTE sequence [TE~ several to tens of microseconds in Cones three-dimensional (3D) UTE] can detect signals from the short T2 and long T2 components in tendons. However, similar acquisition at 2.2 ms mostly detects the long T2 components of the tendons. Specifically, the short component T2* from previous bicomponent fitting analyses ranges between 0.6 to 1.8 ms. Considering an average short component T2* of 1.2 ms (mean of 0.6 and 1.8) (21,24-28). However, similar acquisition at 2.2 ms mostly detects the long

T2 components of the tendons. Specifically, the short component T2* from previous bicomponent fitting analyses ranges between 0.6 to 1.8 ms. Considering an average short component T2* of 1.2 ms (mean of 0.6 and 1.8). These phenomena are anticipated to occur with aging and with potential tendon degeneration which may be associated with the progression of bone disease (4).

The objective of this study is to investigate the differences in apparent long T2 signal fraction (aFrac-LongT2) of the ATTs and PTTs, between female OPe patients, OPo patients, and subjects with normal bone (Normal). We present this article in accordance with the STROBE reporting checklist (available at https://qims.amegroups.com/article/view/10.21037/qims-23-1341/rc).

Methods

Participants' recruitment

Female patients were exclusively enrolled in this study as it is well known that there are sex-based differences in tendon and bone biology (29-31). Fourteen female patients with OPe (72±6 years), thirty-one female patients with OPo (73±6 years), and thirty female subjects with normal bone (Normal, 35±18 years), were recruited. The participants were recruited using flyers distributed in flyers in Radiology, Orthopedics, and Endocrinology clinics at the University of California, San Diego. All individuals must be willing and able to complete 1 hour MRI in the supine position. Individuals with trauma and significant leg and hip injuries within the past 12 months were excluded. The inclusion criteria for each group were as follows: (I) Normal group: pre-menopausal female subjects under 40 years of age or post-menopausal female subjects with a recent T-score above –1; (II) OPe group: post-menopausal female patients with T-scores between –2.5 and –1; and (III) OPo group: post-menopausal female patients with T-scores below –2.5. The study was conducted in accordance with the Declaration of Helsinki (as revised in 2013). The study was approved by the institutional review board (IRB) of the University of California, San Diego (No. 151622), and written informed consent was taken from all individual participants.

UTE-MRI scanning

The lower leg of each participant was scanned on a 3T MRI (MR750, GE Healthcare Technologies, WI, USA) machine using a standard 8-channel (transmit/receive) knee coil. All healthy volunteers ambulatory leg laterality was self-selected. For post-menopausal patients, the leg selection had to match the available side in the hip DXA scan reports, however for patients with both sides DXA reports, the most affected side was selected. The subjects were examined in a feet-first supine position with fully extended knee joint. A cushion was placed outside the coil under the calcaneus after the most comfortable flexion and rotation angle of the ankle joint were decided by the subjects. The imaging slab was centered in the midshaft of the tibia. A non-fat sat dual-echo 3D UTE Cones sequence employs a short rectangular excitation pulse (duration =150 μs) followed by 3D spiral trajectories (conical shape) for k-space acquisition (repetition time =100 ms, TE =0.032 and 2.2 ms, flip angle =45°, bandwidth =125 kHz) was performed for aFrac-LongT2 measurement, which is equal to the 2nd TE signal divided by the UTE signal. The field-of-view (FOV), number of slices, in-plane matrix dimension and slice thickness were 14 cm, 24, 160×160, and 5 mm, respectively. The scan time was approximately 5 minutes.

Mean aFrac-LongT2 was calculated within regions of interest (ROIs) covering the ATTs and PTTs selected by three experienced MRI data analysts using the Image Processing Toolbox in MATLAB software (version 2021, Mathworks, Natick, MA, USA). The selected ROIs were used to calculate the cross-sectional area of the tendons by counting the covered pixels. For quality control purposes, the ATT and PTT boundaries selected for the first five datasets by the readers were confirmed by a board-certified musculoskeletal (MSK) radiologist. Intraclass correlation coefficients (ICCs) were calculated for aFrac-LongT2 and CSA across all data analyzed by the three independent readers. The readers had one to three years of experience in MRI image reading.

Statistical analysis

The one-sample Kolmogorov-Smirnov test results suggested that the aFrac-LongT2 was not normally distributed, therefore the one-way Kruskal-Wallis test by ranks was used to examine the differences in ATTs and PTTs between the three participating groups (Normal, OPe, and OPo). P values below 0.05 were considered as significant. The significance level was corrected using the Holm-Bonferroni method for multiple comparisons between groups. Statistical analysis was performed using MATLAB software.

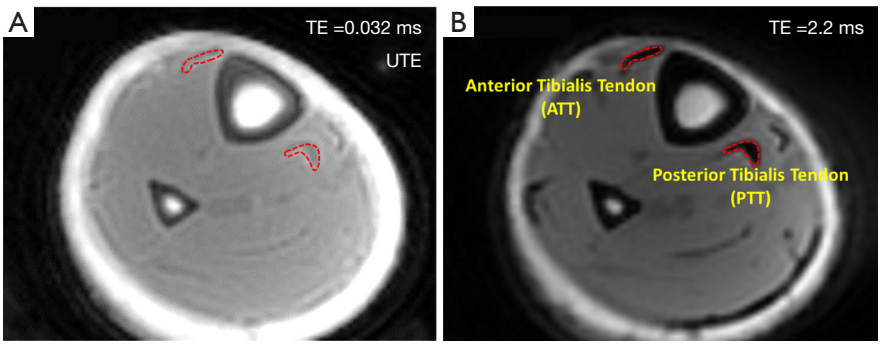

Figure 1 Representative axial images of the ATT and PTT of a healthy 25-year-old female subject. (A) Axial image acquired with UTE Cones MRI sequence (TE =0.032 ms). (B) Axial image acquired with Cones MRI sequence at TE =2.2 ms. Representative ROIs for the anterior and posterior tibialis tendons (ATT and PTT) were selected at TE =2.2 ms as it provided higher contrast (indicated by the red dashed boundary). TE, echo time; UTE, ultrashort echo time; ATT, anterior tibialis tendon; PTT, posterior tibialis tendon; MRI, magnetic resonance imaging; ROI, region of interest.

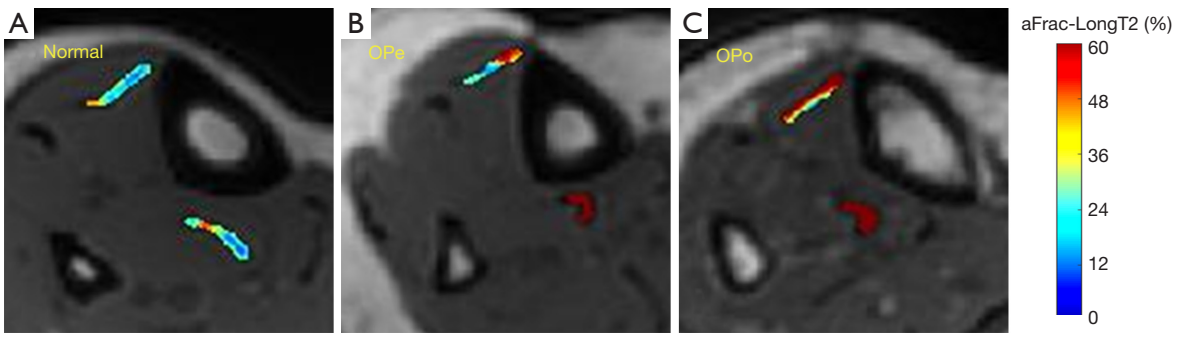

Figure 2 Generated aFrac-LongT2 pixel maps over the ATTs and PTTs for representative subjects in studied groups. (A) aFrac-LongT2 pixel map in a normal subject (28-year-old female). (B) aFrac-LongT2 pixel map in an OPe subject (75-year-old female). (C) aFrac-LongT2 pixel map in an OPo subject (85-year-old female). aFrac-LongT2 in tendons was clearly higher in the OPe and OPo patients than in the Normal participant. OPe, osteopenia; OPo, osteoporosis; aFrac-LongT2, apparent long T2 signal fraction; ATT, anterior tibialis tendon; PTT, posterior tibialis tendon.

Results

UTE (TE =0.032 ms) and second echo (TE =2.2 ms) axial images of the lower leg of a healthy subject are presented in *Figure 1*. While the UTE image detects a high signal in tendons, it lacks adequate contrast to be used for the selection of the tendon ROIs. The second echo image (*Figure 1B*) was used by the data analysts to select ROIs covering the ATTs and PTTs.

Figure 2 shows aFrac-LongT2 maps generated over ATTs and PTTs of three representative Normal, OPe, and OPo subjects. For these examples, aFrac-LongT2 was clearly higher for OPe and OPo patients compared with the Normal participant.

Table 1 summarizes the estimated mean and standard deviation (SD) values of aFrac-LongT2 and CSA in the ATTs and PTTs of participants from the Normal, OPe, and OPo groups. ICC was higher than 0.95 indicating a high level of consistency between the readers. Mean and SD values of body mass index (BMI) and age for subjects in each group are presented in *Table 1*.

The percentage differences and statistical significances of aFrac-LongT2 and CSA between the Normal, OPe, and OPo groups are presented in *Table 2*. aFrac-LongT2 in the ATTs and the PTTs were significantly higher for the OPo group than in the Normal group. The Normal/OPo difference was larger in the PTTs than in the ATTs (22.2% and 34.8% in the ATT and PTT, respectively). CSA in the ATTs was

Table 1 aFrac-LongT2 (%) and CSA (mm^2) in the ATTs and the PTTs for Normal, OPe, and OPo groups

Variables	Normal	OPe	OPo	ICC
Age (years)	35.1±18.1	72.3±6.9	73.0±6.4	–
BMI (kg/m^2)	23.2±4.3	25.8±6.2	22.0±3.8	–
ATT				
aFrac-LongT2 (%)	40.4±10.3	47.5±12.2	49.4±12.3	0.96±0.03
CSA (mm^2)	27.2±8.0	30.3±9.8	35.1±9.4	0.91±0.05
PTT				
aFrac-LongT2 (%)	31.4±6.9	37.1±10.2	42.3±12.2	0.97±0.03
CSA (mm^2)	28.7±8.8	29.9±8.2	33.9±11.2	0.92±0.06

The value is presented as means ± SD. aFrac-LongT2, apparent long T2 signal fraction; CSA, cross-sectional area; ATT, anterior tibialis tendon; PTT, posterior tibialis tendon; OPe, osteopenia; OPo, osteoporosis; ICC, intraclass correlation coefficients; BMI, body mass index.

Table 2 Average differences in percentage as well as the Kruskal-Wallis test results of aFrac-LongT2 and CSA between the studied groups

ROI	Variables	Normal/OPe		Normal/OPo		OPe/OPo	
		Difference (%)	P	Difference (%)	P	Difference (%)	P
ATT	aFrac-LongT2	17.7	0.13	22.2	<0.01	3.9	0.92
	CSA	11.3	0.53	28.7	<0.01	15.6	0.27
PTT	aFrac-LongT2	18.1	0.25	34.8	<0.01	14.1	0.35
	CSA	4.2	0.94	17.9	0.18	13.2	0.54

$\text{Normal/OPo difference} = \frac{\text{aFrac-LongT2 OPo} - \text{aFrac-LongT2 Normal}}{\text{aFrac-LongT2 Normal}} \times 100\%$. aFrac-LongT2, apparent long T2 signal fraction; CSA, cross-sectional area; OPe, osteopenia; OPo, osteoporosis; ROI, region of interest; ATT, anterior tibialis tendon; PTT, posterior tibialis tendon.

significantly higher for the OPo group than in the Normal group (Normal/OPo difference was 28.7, P<0.01). Such a difference for PTTs did not reach the significance level. aFrac-LongT2 and CSA showed a higher trend in the OPe group compared with the Normal group for both ATTs and PTTs, although the differences did not reach statistical significance after the Holm-Bonferroni correction. aFrac-LongT2 and CSA showed a higher trend in the OPo group compared with the OPe group, however, the differences were not significant.

Figure 3 demonstrates the mean, median, SD, and the first and third quartiles of aFrac-LongT2 and CSA for each studied group using box and whisker plots. The dashed lines between groups, indicated with an asterisk, refers to statistically significant differences.

Discussion

This study investigated the differences in aFrac-LongT2 of ATTs and PTTs between OPo, OPe, and Normal subjects. aFrac-LongT2 is an estimation of the proton pools with long T2 in tendons divided by the total proton pool. aFrac-LongT2 was calculated using a rapid dual-echo UTE MRI sequence which generally takes under five minutes to acquire. Such a rapid UTE-MRI-based technique for quantitative tendon evaluation can be considered translatable into the clinical workflow due to its simplicity and time efficiency.

Notably, the required time for dual-echo UTE MRI sequence depends on the acquisition techniques. For example, two-dimensional (2D) UTE acquisition (32,33) is faster than a three-dimensional (3D) acquisition (using radial, spiral, or cones trajectories) (22,34), while among the 3D acquisitions, the spiral or Cones is faster than a radial technique. Moreover, the UTE scan time can be improved by several acceleration techniques such as the stretching spokes in Cones (35), compressed sensing (36-38), and parallel imaging (39,40). Since the proposed method here for aFrac-LongT2 at most requires two acquisitions

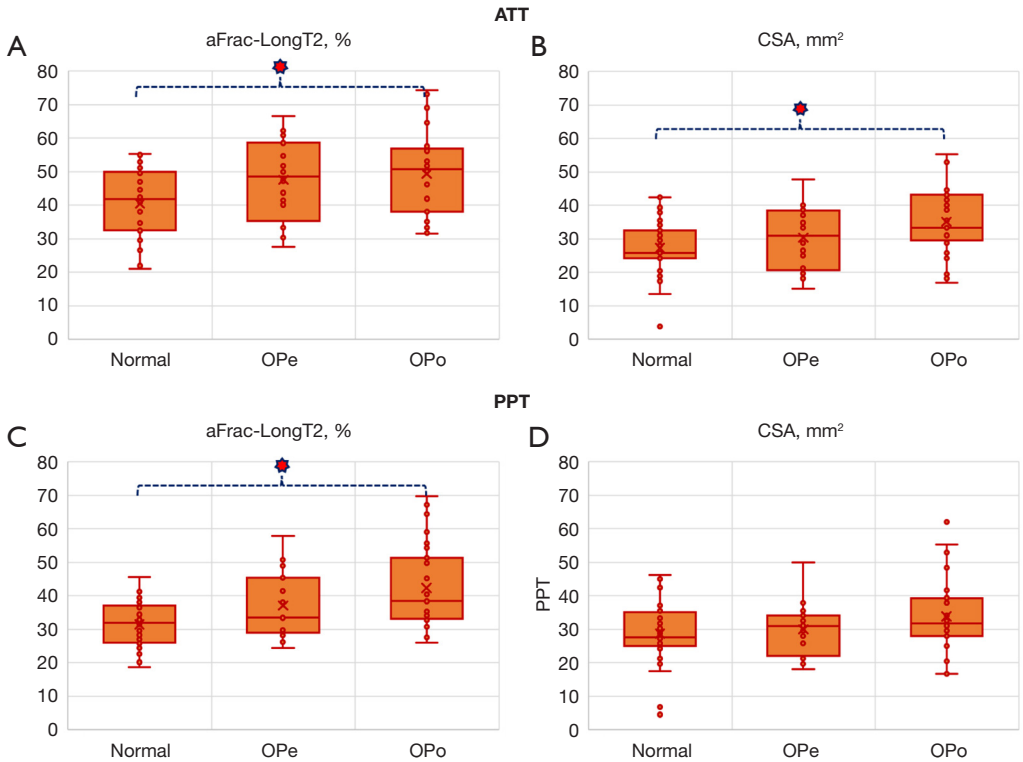

Figure 3 Mean aFrac-LongT2 and CSA for Normal, OPe, and OPo groups. (A) Box-whisker plot of aFrac-LongT2 in ATTs. (B) Box-whisker plot of CSA in ATTs. (C) Box-whisker plot of aFrac-LongT2 in PTTs. (D) Box-whisker plot of CSA in PTTs. The central line and the cross-point in each plot indicate the median and mean values, respectively. The upper and lower edges of the box indicate the first and third quartiles, respectively. aFrac-LongT2 was significantly higher in OPo patients than the Normal group for both the ATTs and PTTs. CSA was significantly higher in the OPo group than the Normal only for ATTs. Asterisks indicate significant difference. ATT, anterior tibialis tendon; aFrac-LongT2, apparent long T2 signal fraction; OPe, osteopenia; OPo, osteoporosis; CSA, cross-sectional area; PTT, posterior tibialis tendon.

(for some resolutions it can be performed as one acquisition), they are likely faster than techniques with multiple acquisitions. Several UTE MRI techniques have been reported in the literature for both *ex vivo* and *in vivo* tendon assessments that utilize multiple acquisitions per exam, including UTE-T2* (17,20,21,27,41-47), UTE-T1 (43,48-51), UTE-T1ρ (52), MT (42,49,50,53-56), and inversion recovery (IR) UTE-T2* (57). The Achilles (18,20,21,41-44,49,51,52,55,56,58,59), rotator cuff (46,53,54), tibialis (49,50), and patellar tendons (44,58,60) are the main targeted tendons for UTE-MRI-based assessments.

aFrac-LongT2 in the ATTs and PTTs were significantly higher for OPo compared with the Normal group (22.2% and 34.8 in ATT and PTT, respectively). Similar ranges of differences were reported in one of our previous studies for MMF reduction (–32.1 ATT and –24.2 for PTT) for the same group of patients (49). However, the UTE technique used in the prior study required 33 minutes of scan time (including the prerequisite T1 measurement and UTE-MT sequence).

aFrac-LongT2 showed a higher trend in the OPe group compared with the Normal group for both ATTs and PTTs, although the differences were not statistically significant. This agreed with the non-significant tendons' MMF reduction revealed previously in OPe patients compared with the Normal group (49). The aFrac-LongT2 differences between the OPe and OPo groups were not significant. Therefore, the proposed MRI techniques may lack the required sensitivity to detect all age- or bone-health-related differences in tendons, particularly with the current imaging setup. Group OPe notably had a higher BMI than other groups, which might result in insignificant differences of aFrac-LongT2 with other groups.

The performance, quality, and composition of tendons are influenced by aging (61-63). Concurrent with age-related changes, OPo-related bone weakening may affect the tendons' quality. In more details, lower levels of insulin-like growth factor-I (IGF-I), growth hormone (GH), and sex steroids can lead to the bone, tendon, and muscle deterioration (6-9,64,65), as they reduce the protein turnover and cell activity in these tissues (1,3,8,66). For example, the rotator cuff tendon's mechanical strength has shown significant correlation to bone mineral density in the humeral head of a rabbit model (4).

The limitations of this study can be summarized in four aspects. First, the subject pool for this study was limited to only female participants to avoid sex-related differences (29-31). Repeating this study on a male patient population and comparisons with the current results will be necessary in the future. Second, a limited number of patients were recruited for the current study, and also there was a control age-matched limitation in this study. Aging can affect the tendons' quality, so a portion of OPe/Normal and OPo/Normal differences might be only age-related. Including a control age-matched group should be considered in future investigations. aFrac-LongT2 should be examined on a larger group of OPe and OPo patients to confirm its clinical applications for tendons assessment in OPo disease monitoring and there is also a need to compare the results with ultrasonography results as the gold standard and check for the sensitivity, specificity, positive predictive value (PPV), and negative predictive value (NPV). Third, the current imaging setup, particularly the resolution with a 0.87×0.87×5 mm^3 voxel size and the small tendon cross-sectional area may result in partial volume artifacts. The potential chemical shift artifacts might also affect the results. Future phantom studies should be performed to optimize the image resolutions and slice thickness for specific tendons of interest. Fourth, the magic angle sensitivity (67-69) of aFrac-LongT2 has not been investigated yet. Although there is limited room for variations in the orientation of the lower leg tendons', utilizing this technique for tendons around joints, that are subject to large orientation changes, may need thorough magic angle sensitivity assessment.

Conclusions

This study investigated the differences in apparent aFrac-LongT2 of the lower leg tendons between OPo, OPe, and Normal subjects. Apparent Frac-LongT2 was calculated using a rapid dual-echo UTE MRI technique and showed potential for the detection and evaluation of changes in the tibialis tendons of the patients with OPo. Apparent Frac-LongT2 showed significantly higher values in the tibialis tendons of the OPo group compared with the Normal group. The results of this study highlight the need for a larger-scale study to further validate the preliminary findings. Tendon insufficiency causes marked discomfort and impairs the balance; therefore tendons are recommended to be evaluated in patients with bone loss to avoid potential debilitating sequela.

Acknowledgments

Funding: This study was supported by grants from the National Institutes of Health (Nos. K01AR080257, R01AR068987, R01AR062581, R01AR075825, R01AR079484, and 5P30AR073761), Veterans Affairs Clinical Science and Rehabilitation R&D (Nos. I01CX001388, I01BX005952, and I01CX000625), and GE Healthcare. GE Healthcare was not involved in the study design, collection, analysis, interpretation of data, the writing of this article or the decision to submit it for publication.

Footnote

Reporting Checklist: The authors have completed the STROBE reporting checklist. Available at https://qims.amegroups.com/article/view/10.21037/qims-23-1341/rc

Conflicts of Interest: All authors have completed the ICMJE uniform disclosure form (available at https://qims.amegroups.com/article/view/10.21037/qims-23-1341/coif). Jiang Du serves as an unpaid editorial board member of *Quantitative Imaging in Medicine and Surgery*. All authors report that this study was supported by GE Healthcare. GE Healthcare was not involved in the study design, collection, analysis, interpretation of data, the writing of this article or the decision to submit it for publication. The authors have no other conflicts of interest to declare.

Ethical Statement: The authors are accountable for all aspects of the work in ensuring that questions related to the accuracy or integrity of any part of the work are appropriately investigated and resolved. The study was conducted in accordance with the Declaration of Helsinki (as revised in 2013). The study was approved by

the institutional review board (IRB) of the University of California, San Diego (No. 151622), and written informed consent was taken from all individual participants.

References

1. Edwards MH, Dennison EM, Aihie Sayer A, Fielding R, Cooper C. Osteoporosis and sarcopenia in older age. Bone 2015;80:126-30.
2. Cederholm T, Cruz-Jentoft AJ, Maggi S. Sarcopenia and fragility fractures. Eur J Phys Rehabil Med 2013;49:111-7.
3. Gumpenberger M, Wessner B, Graf A, Narici MV, Fink C, Braun S, Hoser C, Blazevich AJ, Csapo R. Remodeling the Skeletal Muscle Extracellular Matrix in Older Age-Effects of Acute Exercise Stimuli on Gene Expression. Int J Mol Sci 2020;21:7089.
4. Chen X, Giambini H, Ben-Abraham E, An KN, Nassr A, Zhao C. Effect of Bone Mineral Density on Rotator Cuff Tear: An Osteoporotic Rabbit Model. PLoS One 2015;10:e0139384.
5. Maffulli N, Cuozzo F, Migliorini F, Oliva F. The tendon unit: biochemical, biomechanical, hormonal influences. J Orthop Surg Res 2023;18:311.
6. Girgis CM, Mokbel N, Digirolamo DJ. Therapies for musculoskeletal disease: can we treat two birds with one stone? Curr Osteoporos Rep 2014;12:142-53.
7. Giustina A, Mazziotti G, Canalis E. Growth hormone, insulin-like growth factors, and the skeleton. Endocr Rev 2008;29:535-59.
8. Tagliaferri C, Wittrant Y, Davicco MJ, Walrand S, Coxam V. Muscle and bone, two interconnected tissues. Ageing Res Rev 2015;21:55-70.
9. Urban RJ. Growth hormone and testosterone: anabolic effects on muscle. Horm Res Paediatr 2011;76 Suppl 1:81-3.
10. Wren TA, Yerby SA, Beaupré GS, Carter DR. Influence of bone mineral density, age, and strain rate on the failure mode of human Achilles tendons. Clin Biomech (Bristol, Avon) 2001;16:529-34.
11. Pierre-Jerome C, Moncayo V, Terk MR. MRI of the Achilles tendon: a comprehensive review of the anatomy, biomechanics, and imaging of overuse tendinopathies. Acta Radiol 2010;51:438-54.
12. Cosman F, de Beur SJ, LeBoff MS, Lewiecki EM, Tanner B, Randall S, Lindsay R; National Osteoporosis Foundation. Clinician's Guide to Prevention and Treatment of Osteoporosis. Osteoporos Int 2014;25:2359-81.
13. Zielinska N, Tubbs RS, Paulsen F, Szewczyk B, Podgórski M, Borowski A, Olewnik Ł. Anatomical Variations of the Tibialis Anterior Tendon Insertion: An Updated and Comprehensive Review. J Clin Med 2021;10:3684.
14. Yao K, Yang TX, Yew WP. Posterior Tibialis Tendon Dysfunction: Overview of Evaluation and Management. Orthopedics 2015;38:385-91.
15. Weinreb JH, Sheth C, Apostolakos J, McCarthy MB, Barden B, Cote MP, Mazzocca AD. Tendon structure, disease, and imaging. Muscles Ligaments Tendons J 2014;4:66-73.
16. Chang EY, Du J, Chung CB. UTE imaging in the musculoskeletal system. J Magn Reson Imaging 2015;41:870-83.
17. Juras V, Zbyn S, Pressl C, Valkovic L, Szomolanyi P, Frollo I, Trattnig S. Regional variations of T_2* in healthy and pathologic achilles tendon in vivo at 7 Tesla: preliminary results. Magn Reson Med 2012;68:1607-13.
18. Du J, Chiang AJ, Chung CB, Statum S, Znamirowski R, Takahashi A, Bydder GM. Orientational analysis of the Achilles tendon and enthesis using an ultrashort echo time spectroscopic imaging sequence. Magn Reson Imaging 2010;28:178-84.
19. Dallaudière B, Trotier A, Ribot E, Verdier D, Lepreux S, Miraux S, Hauger O. Three-dimensional ultrashort echo time (3D UTE) MRI of Achilles tendon at 4.7T MRI with comparison to conventional sequences in an experimental murine model of spondyloarthropathy. J Magn Reson Imaging 2019;50:127-35.
20. Chang EY, Du J, Bae WC, Statum S, Chung CB. Effects of Achilles tendon immersion in saline and perfluorochemicals on T2 and T2*. J Magn Reson Imaging 2014;40:496-500.
21. Robson MD, Benjamin M, Gishen P, Bydder GM. Magnetic resonance imaging of the Achilles tendon using ultrashort TE (UTE) pulse sequences. Clin Radiol 2004;59:727-35.
22. Ma Y, Jang H, Jerban S, Chang EY, Chung CB, Bydder GM, Du J. Making the invisible visible-ultrashort echo

time magnetic resonance imaging: Technical developments and applications. Appl Phys Rev 2022;9:041303.
23. Rajapakse CS, Bashoor-Zadeh M, Li C, Sun W, Wright AC, Wehrli FW. Volumetric Cortical Bone Porosity Assessment with MR Imaging: Validation and Clinical Feasibility. Radiology 2015;276:526-35.
24. Grosse U, Syha R, Hein T, Gatidis S, Grözinger G, Schabel C, Martirosian P, Schick F, Springer F. Diagnostic value of T1 and T2 * relaxation times and off-resonance saturation effects in the evaluation of Achilles tendinopathy by MRI at 3T. J Magn Reson Imaging 2015;41:964-73.
25. Gärdin A, Rasinski P, Berglund J, Shalabi A, Schulte H, Brismar TB. T2 * relaxation time in Achilles tendinosis and controls and its correlation with clinical score. J Magn Reson Imaging 2016;43:1417-22.
26. Chang EY, Du J, Iwasaki K, Biswas R, Statum S, He Q, Bae WC, Chung CB. Single- and Bi-component T2* analysis of tendon before and during tensile loading, using UTE sequences. J Magn Reson Imaging 2015;42:114-20.
27. Liu J, Nazaran A, Ma Y, Chen H, Zhu Y, Du J, Li S, Zhou Q, Zhao Y. Single- and Bicomponent Analyses of T2* Relaxation in Knee Tendon and Ligament by Using 3D Ultrashort Echo Time Cones (UTE Cones) Magnetic Resonance Imaging. Biomed Res Int 2019;2019:8597423.
28. Chang EY, Du J, Statum S, Pauli C, Chung CB. Quantitative bi-component T2* analysis of histologically normal Achilles tendons. Muscles Ligaments Tendons J 2015;5:58-62.
29. Sarver DC, Kharaz YA, Sugg KB, Gumucio JP, Comerford E, Mendias CL. Sex differences in tendon structure and function. J Orthop Res 2017;35:2117-26.
30. Pease LI, Clegg PD, Proctor CJ, Shanley DJ, Cockell SJ, Peffers MJ. Cross platform analysis of transcriptomic data identifies ageing has distinct and opposite effects on tendon in males and females. Sci Rep 2017;7:14443.
31. Patton DM, Bigelow EMR, Schlecht SH, Kohn DH, Bredbenner TL, Jepsen KJ. The relationship between whole bone stiffness and strength is age and sex dependent. J Biomech 2019;83:125-33.
32. Harkins KD, Ketsiri T, Nyman JS, Does MD. Fast bound and pore water mapping of cortical bone with arbitrary slice oriented two-dimensional ultra-short echo time. Magn Reson Med 2023;89:767-73.
33. Manhard MK, Harkins KD, Gochberg DF, Nyman JS, Does MD. 30-Second bound and pore water concentration mapping of cortical bone using 2D UTE with optimized half-pulses. Magn Reson Med 2017;77:945-50.
34. Afsahi AM, Ma Y, Jang H, Jerban S, Chung CB, Chang EY, Du J. Ultrashort Echo Time Magnetic Resonance Imaging Techniques: Met and Unmet Needs in Musculoskeletal Imaging. J Magn Reson Imaging 2022;55:1597-612.
35. Wan L, Ma Y, Yang J, Jerban S, Searleman AC, Carl M, Le N, Chang EY, Tang G, Du J. Fast quantitative three-dimensional ultrashort echo time (UTE) Cones magnetic resonance imaging of major tissues in the knee joint using extended sprial sampling. NMR Biomed 2020;33:e4376.
36. Athertya JS, Ma Y, Masoud Afsahi A, Lombardi AF, Moazamian D, Jerban S, Sedaghat S, Jang H. Accelerated Quantitative 3D UTE-Cones Imaging Using Compressed Sensing. Sensors (Basel) 2022;22:7459.
37. Uecker M, Lai P, Murphy MJ, Virtue P, Elad M, Pauly JM, Vasanawala SS, Lustig M. ESPIRiT--an eigenvalue approach to autocalibrating parallel MRI: where SENSE meets GRAPPA. Magn Reson Med 2014;71:990-1001.
38. Lustig M, Donoho D, Pauly JM. Sparse MRI: The application of compressed sensing for rapid MR imaging. Magn Reson Med 2007;58:1182-95.
39. Otazo R, Kim D, Axel L, Sodickson DK. Combination of compressed sensing and parallel imaging for highly accelerated first-pass cardiac perfusion MRI. Magn Reson Med 2010;64:767-76.
40. Chang G, Deniz CM, Honig S, Rajapakse CS, Egol K, Regatte RR, Brown R. Feasibility of three-dimensional MRI of proximal femur microarchitecture at 3 tesla using 26 receive elements without and with parallel imaging. J Magn Reson Imaging 2014;40:229-38.
41. Chang EY, Bae WC, Statum S, Du J, Chung CB. Effects of repetitive freeze-thawing cycles on T2 and T2 of the Achilles tendon. Eur J Radiol 2014;83:349-53.
42. Chen B, Cheng X, Dorthe EW, Zhao Y, D'Lima D, Bydder GM, Liu S, Du J, Ma YJ. Evaluation of normal cadaveric Achilles tendon and enthesis with ultrashort echo time (UTE) magnetic resonance imaging and indentation testing. NMR Biomed 2019;32:e4034.
43. Filho GH, Du J, Pak BC, Statum S, Znamorowski R, Haghighi P, Bydder G, Chung CB. Quantitative characterization of the Achilles tendon in cadaveric specimens: T1 and T2* measurements using ultrashort-TE MRI at 3 T. AJR Am J Roentgenol 2009;192:W117-24.
44. Juras V, Apprich S, Szomolanyi P, Bieri O, Deligianni X, Trattnig S. Bi-exponential T2 analysis of healthy and diseased Achilles tendons: an in vivo preliminary magnetic resonance study and correlation with clinical score. Eur Radiol 2013;23:2814-22.
45. Chang EY, Szeverenyi NM, Statum S, Chung CB. Rotator cuff tendon ultrastructure assessment with reduced-

orientation dipolar anisotropy fiber imaging. AJR Am J Roentgenol 2014;202:W376-8.
46. Xie Y, Liu S, Qu J, Wu P, Tao H, Chen S. Quantitative Magnetic Resonance Imaging UTE-T2* Mapping of Tendon Healing After Arthroscopic Rotator Cuff Repair: A Longitudinal Study. Am J Sports Med 2020;48:2677-85.
47. Jerban S, Nazaran A, Carl M, Cheng X, Chang EY, Du J. (ISMRM 2017) The effect of loading on T2* and MT ratio in tendons: A feasibility study. [cited 2023 Nov 21]. Available online: https://archive.ismrm.org/2017/1535.html
48. Chen B, Zhao Y, Cheng X, Ma Y, Chang EY, Kavanaugh A, Liu S, Du J. Three-dimensional ultrashort echo time cones (3D UTE-Cones) magnetic resonance imaging of entheses and tendons. Magn Reson Imaging 2018;49:4-9.
49. Jerban S, Ma Y, Afsahi AM, Lombardi A, Wei Z, Shen M, Wu M, Le N, Chang DG, Chung CB, Du J, Chang EY. Lower Macromolecular Content in Tendons of Female Patients with Osteoporosis versus Patients with Osteopenia Detected by Ultrashort Echo Time (UTE) MRI. Diagnostics (Basel) 2022;12:1061.
50. Jerban S, Ma Y, Namiranian B, Ashir A, Shirazian H, Wei Z, Le N, Wu M, Cai Z, Du J, Chang EY. Age-related decrease in collagen proton fraction in tibial tendons estimated by magnetization transfer modeling of ultrashort echo time magnetic resonance imaging (UTE-MRI). Sci Rep 2019;9:17974.
51. Wright P, Jellus V, McGonagle D, Robson M, Ridgeway J, Hodgson R. Comparison of two ultrashort echo time sequences for the quantification of T1 within phantom and human Achilles tendon at 3 T. Magn Reson Med 2012;68:1279-84.
52. Du J, Carl M, Diaz E, Takahashi A, Han E, Szeverenyi NM, Chung CB, Bydder GM. Ultrashort TE T1rho (UTE T1rho) imaging of the Achilles tendon and meniscus. Magn Reson Med 2010;64:834-42.
53. Zhu Y, Cheng X, Ma Y, Wong JH, Xie Y, Du J, Chang EY. Rotator cuff tendon assessment using magic-angle insensitive 3D ultrashort echo time cones magnetization transfer (UTE-Cones-MT) imaging and modeling with histological correlation. J Magn Reson Imaging 2018;48:160-8.
54. Ashir A, Ma Y, Jerban S, Jang H, Wei Z, Le N, Du J, Chang EY. Rotator Cuff Tendon Assessment in Symptomatic and Control Groups Using Quantitative MRI. J Magn Reson Imaging 2020;52:864-72.
55. Fang Y, Zhu D, Wu W, Yu W, Li S, Ma YJ. Assessment of Achilles Tendon Changes After Long-Distance Running Using Ultrashort Echo Time Magnetization Transfer MR Imaging. J Magn Reson Imaging 2022;56:814-23.
56. Hodgson RJ, Evans R, Wright P, Grainger AJ, O'Connor PJ, Helliwell P, McGonagle D, Emery P, Robson MD. Quantitative magnetization transfer ultrashort echo time imaging of the Achilles tendon. Magn Reson Med 2011;65:1372-6.
57. Ma YJ, Zhu Y, Lu X, Carl M, Chang EY, Du J. Short T(2) imaging using a 3D double adiabatic inversion recovery prepared ultrashort echo time cones (3D DIR-UTE-Cones) sequence. Magn Reson Med 2018;79:2555-63.
58. Qiao Y, Tao HY, Ma K, Wu ZY, Qu JX, Chen S. UTE-T2(∗) Analysis of Diseased and Healthy Achilles Tendons and Correlation with Clinical Score: An In Vivo Preliminary Study. Biomed Res Int 2017;2017:2729807.
59. Moazamian D, Athertya JS, Dwek S, Lombardi AF, Mohammadi HS, Sedaghat S, Jang H, Ma Y, Chung CB, Du J, Jerban S, Chang EY. Achilles tendon and enthesis assessment using ultrashort echo time magnetic resonance imaging (UTE-MRI) T1 and magnetization transfer (MT) modeling in psoriatic arthritis. NMR Biomed 2024;37:e5040.
60. Agergaard AS, Malmgaard-Clausen NM, Svensson RB, Nybing JD, Boesen M, Kjaer M, Magnusson SP, Hansen P. UTE T2* mapping of tendinopathic patellar tendons: an MRI reproducibility study. Acta Radiol 2021;62:215-24.
61. Carroll CC, Dickinson JM, Haus JM, Lee GA, Hollon CJ, Aagaard P, Magnusson SP, Trappe TA. Influence of aging on the in vivo properties of human patellar tendon. J Appl Physiol (1985) 2008;105:1907-15.
62. Kannus P, Paavola M, Józsa LX. Aging and Degeneration of Tendons. In: Maffulli, N., Renström P, Leadbetter WB. editros Tendon Injuries. Springer, London, 2005. Available online: https://doi.org/10.1007/1-84628-050-8_4
63. Svensson RB, Heinemeier KM, Couppé C, Kjaer M, Magnusson SP. Effect of aging and exercise on the tendon. J Appl Physiol (1985) 2016;121:1237-46.
64. Yoshida T, Delafontaine P. Mechanisms of IGF-1-Mediated Regulation of Skeletal Muscle Hypertrophy and Atrophy. Cells 2020;9:1970.
65. Reginster JY, Beaudart C, Buckinx F, Bruyère O. Osteoporosis and sarcopenia: two diseases or one? Curr Opin Clin Nutr Metab Care 2016;19:31-6.
66. Frizziero A, Vittadini F, Gasparre G, Masiero S. Impact of oestrogen deficiency and aging on tendon: concise review. Muscles Ligaments Tendons J 2014;4:324-8.
67. Shao H, Pauli C, Li S, Ma Y, Tadros AS, Kavanaugh A, Chang EY, Tang G, Du J. Magic angle effect plays a major role in both T1rho and T2 relaxation in articular cartilage.

Osteoarthritis Cartilage 2017;25:2022-30.
68. Wu M, Ma Y, Wan L, Jerban S, Jang H, Chang EY, Du J. Magic angle effect on adiabatic T(1ρ) imaging of the Achilles tendon using 3D ultrashort echo time cones trajectory. NMR Biomed 2020;33:e4322.
69. Wu M, Ma YJ, Kasibhatla A, Chen M, Jang H, Jerban S, Chang EY, Du J. Convincing evidence for magic angle less-sensitive quantitative T(1ρ) imaging of articular cartilage using the 3D ultrashort echo time cones adiabatic T(1ρ) (3D UTE cones-AdiabT(1ρ)) sequence. Magn Reson Med 2020;84:2551-60.

Cite this article as: Jerban S, Moazamian D, Ma Y, Afsahi AM, Dwek S, Athertya J, Malhi B, Jang H, Woods G, Chung CB, Du J, Chang EY. Fast dual-echo estimation of apparent long T2 fraction using ultrashort echo time magnetic resonance imaging in tibialis tendons and its osteoporosis-related differences in women. Quant Imaging Med Surg 2024;14(4):3146-3156. doi: 10.21037/qims-23-1341

